

LASER INDUCED PERIODIC SURFACE STRUCTURING FOR SURFACE  
ENHANCED RAMAN SPECTROSCOPY

A THESIS SUBMITTED TO  
THE GRADUATE SCHOOL OF NATURAL AND APPLIED SCIENCES  
OF  
MIDDLE EAST TECHNICAL UNIVERSITY

BY  
ZEYNEP TUĞÇE ÖZKARSLIGİL

IN PARTIAL FULFILLMENT OF THE REQUIREMENTS  
FOR  
THE DEGREE OF MASTER OF SCIENCE  
IN  
PHYSICS

JANUARY 2020

Approval of the thesis:

**LASER INDUCED PERIODIC SURFACE STRUCTURING FOR SURFACE  
ENHANCED RAMAN SPECTROSCOPY**

submitted by **ZEYNEP TUĞÇE ÖZKARSLIĞIL** in partial fulfillment of the requirements for the degree of **Master of Science in Physics, Middle East Technical University** by,

Prof. Dr. Halil Kalıpçılar  
Dean, Graduate School of **Natural and Applied Sciences**

\_\_\_\_\_

Prof. Dr. Altuğ Özpineci  
Head of the Department, **Physics**

\_\_\_\_\_

Assoc. Prof. Dr. Alpan Bek  
Supervisor, **Physics, METU**

\_\_\_\_\_

Assist. Prof. Dr. Ihor Pavlov  
Co-Supervisor, **Physics, METU**

\_\_\_\_\_

**Examining Committee Members:**

Assoc. Prof. Dr. Emren Nalbant Esentürk  
Chemistry, METU

\_\_\_\_\_

Assoc. Prof. Dr. Alpan Bek  
Physics, METU

\_\_\_\_\_

Assist. Prof. Dr. Ihor Pavlov  
Physics, METU

\_\_\_\_\_

Prof. Dr. Okan Esentürk  
Chemistry, METU

\_\_\_\_\_

Assoc. Prof. Dr. Mehmet Emre Taşgın  
Institute of Nuclear Science, Hacettepe Uni.

\_\_\_\_\_

Date: 31.01.2020



**I hereby declare that all information in this document has been obtained and presented in accordance with academic rules and ethical conduct. I also declare that, as required by these rules and conduct, I have fully cited and referenced all material and results that are not original to this work.**

Name, Last name : Zeynep Tuğçe Özkarslıgil

Signature :

## **ABSTRACT**

### **LASER INDUCED PERIODIC SURFACE STRUCTURING FOR SURFACE ENHANCED RAMAN SPECTROSCOPY**

Özkarşılıgil, Zeynep Tuğçe

Master of Science, Physics

Supervisor: Assoc. Prof. Dr. Alpan Bek

Co-Supervisor: Assist. Prof. Dr. Ihor Pavlov

January 2020, 45 pages

In this study, our aim is to fabricate and characterize efficient substrates of surface enhanced Raman spectroscopy (SERS) utilizing the field enhancement due to hot spots made by recently developed method of laser induced periodic surface structuring (LIPSS). LIPSS is a cost-effective technique for rapid processing of almost any materials compared to conventional lithography methods. Coating of a thin silver film on LIPSS applied substrate surface provides to observe the localized surface plasmon effect for SERS measurement with the use of Raman reporter molecules interacting with silver substrate at the plasmon frequency. In order to characterize the optical properties, diffuse and total reflectivity of the substrates will be measured. Among possible expected applications of such prepared substrates are photonic templates for thin film optoelectronic devices with strong field enhancement properties.

**Keywords:** Surface enhanced Raman scattering, Laser induced periodic surface structures

## ÖZ

### LASERLİ PERİYODİK YÜZEY YAPILANDIRILMA İLE YÜZEY ARTIRIMLI RAMAN SAÇILMASI

Özkarslıgil, Zeynep Tuğçe  
Yüksek Lisans, Fizik  
Tez Yöneticisi: Doç. Dr. Alpan Bek  
Ortak Tez Yöneticisi: Dr. Öğr. Üyesi Ihor Pavlov

Ocak 2020, 45 sayfa

Bu çalışmada amacımız, laserle periyodik yüzey yapılandırılmış sıcak noktaların oluşturduğu alan artırımını kullanarak yüzey artırılmış Raman spektroskopi için verimli alttaş yüzeyleri üretmek ve karakterize etmektir. Laserle periyodik yüzey yapılandırma hemen hemen bütün malzemelerde hızlı bir şekilde uygulanabilen, kullarımdaki diğer lithografi tekniklerine göre düşük maliyetli bir tekniktir. LIPSS uygulanan yüzeylerin gümüş ile kaplanması yerel plazmon etkisinin gözlemlenmesini ve Raman aktif moleküllerinin saçılmalarıyla gümüş yapıdaki plazmonların etkileşime girmesini sağlamaktadır. Bu şekilde hazırlanan yüzeylerin optik özelliklerini karakterize etmek için, substratların dağınık ve toplam yansıtıcılıkları ölçülecektir. Bu gibi hazırlanan alttaşların beklenen uygulamaları arasında, ince film optoelektronik cihazlar için güçlü alan artırıcı özelliklere sahip fotonik şablonlar bulunur.

Anahtar Kelimeler: Yüzey artırımı Raman saçılması, Laserle şekillendirilmiş periyodik yüzey

*To My Father*

## ACKNOWLEDGMENTS

First and foremost, I am indebted to my supervisor Assoc. Prof Dr. Alpan Bek for his dedicated help, great patience, and continuous support. He has been a role model not only because his impeccable knowledge, but also positive attitude that have always kept me motivated.

I would also like to extend my deepest gratitude to my co-advisor Asisst. Prof. Dr. Ihor Pavlov for his immense knowledge in the fields of lasers and optics and for his enthusiasm. This research behind it would not have been possible without the exceptional support of him. His attention to detail have been an inspiration.

I would like to thank Prof. Dr. Rařit Turan for giving me the opportunity of working in GÜNAM laboratories.

I would like to thanks Zafer ılgın for his motivation and being always by side me and Samet Özdemir for his continous support and help, E. Hande iftınar for to be supported by a wonderful woman, İ Murat Öztürk, Gence Bektař, Wiria Soltanpoor and Milad Ghasemi and Mete Günöven and Emre Demirezen for being always positive and helpful They have been great teamworkers and have always elevated me.

I cannot express enough thanks to Namık Aan for his continuous support and encouragement.

I would like to express my special thanks of gratitude to Prof. Dr. Bayram Tekin. He has been adorable mentor and a role model. I have benefited tremendously from his ingenious suggestions and excellent guidance. I could not have imagined having a better mentor.

I also want to thank my family to my mom, Seher Özkarslıgil, my sister and my first teacher Tuba Özkarslıgil, my brother Dogan Özkarslıgil and my best friend and brother Ahmet Özkarslıgil. Also, my friends who make me feel like my family, Ayřegöl Gümüş and M. Akif Fındıklı They make my life more cheerful.

## TABLE OF CONTENTS

ABSTRACT.....	v
ÖZ.....	vi
ACKNOWLEDGMENTS .....	viii
TABLE OF CONTENTS.....	ix
LIST OF TABLES .....	xi
LIST OF FIGURES .....	xii
LIST OF ABBREVIATIONS .....	xiii
1. INTRODUCTION .....	1
2. THEORETICAL FRAMEWORK.....	5
2.1 Surface Plasmon Polariton and Plasma Frequency.....	5
2.1.1 Condition for Excitation of the Surface Plasmon Polariton.....	8
2.1.2 Phase- Matching.....	11
2.2 Localized SP.....	11
2.3 Laser Induced Periodic Surface Structures .....	13
2.4 Surface Enhanced Raman Scattering .....	15
2.4.1 Raman Scattering .....	16
2.4.2 Enhancement Factor.....	18
3. EXPERIMENTAL METHODS.....	21
3.1 Preparation of Substrates.....	21
3.2 Laser Induced Periodic Surface Structure Formation .....	24
3.3 SEM as An Analysis Tools .....	26
3.4 Angle Resolved Scattering .....	27

3.5	Raman Measurement .....	28
4.	RESULTS AND DISCUSSION.....	31
4.1	SEM Images of LIPSS .....	31
4.2	Angle Resolved Scattering.....	33
4.3	RAMAN.....	36
5.	CONCLUSION .....	41
	REFERENCES .....	43

## **LIST OF TABLES**

Table 3-1 Thickness and type of the metallic interlayer of the SERS substrate..... 23

## LIST OF FIGURES

<i>Figure 2.1. The surface plasmon polariton on the interface between a dielectric and a metal surface is similar to electromagnetic wave propagation on boundary .</i>	8
<i>Figure 2.2 Plane wave interaction with metal surface.....</i>	11
<i>Figure 2.3 Jablonski Diagram .....</i>	16
<i>Figure 3.1 Configuration of the layers of the SERS substrate .....</i>	21
<i>Figure 3.2 Steps involved in the preparation of SERS substrate .....</i>	23
<i>Figure 3.3 Gratings by LIPSS on the 200 nm thicken titanium surface.....</i>	26
<i>Figure 3.4 Experimental Configuration of Angular Resolved Scattering .....</i>	28
<i>Figure 3.5 Raman Spectroscopy Set up for the measurement of SERS.....</i>	29
<i>Figure 4.1 Some forms obtained in a and c perpendicular polarization is used in b both perpendicular and parallel polarization are used succesively. Texture in a and b is formed on Ti in c it is Mo surface. ....</i>	32
<i>Figure 4.2 Angle resolved scattering and the diffraction pattern of the grating processed by LIPSS on Ti surface. ....</i>	33
<i>Figure 4.3 Reflection of laser from the grating structured surface by LIPSS. Line A is normal incidence used for finding the period of the grating and Line B refers to reflection with 20° incidence angle. ....</i>	34
<i>Figure 4.4 The periods found via Gwyddion Software.....</i>	35
<i>Figure 4.5 Raman spectrum of 10<sup>-4</sup> M CV liquid droplet on Si wafer .....</i>	36
<i>Figure 4.6 Peak area around 1350 cm<sup>-1</sup> used for calculation of the CV dye molecule used SERS intensity spectra of Mo grating surfaces coated by Ag film. Exposure time 5 s and accumulation is 10. ....</i>	37
<i>Figure 4.7 Enhancement of 20 nm Ag thin films on LIPSS applied 400 nm thicken Mo surface .....</i>	38
<i>Figure 4.8 Variously structured Mo surfaces, most powerful signal obtained in larger band correspond to more roughened surface considering the scanning speed. ....</i>	39

## LIST OF ABBREVIATIONS

SP	Surface Plasmon
SPP	Surface Plasmon Polariton
LSP	Localized Surface Plasmon
LIPSS	Laser Induced Periodic Surface Structuring
SERS	Surface Enhanced Raman Spectroscopy
SEM	Scanning Electron Microscopy
ARS	Angle Resolved Scattering



## CHAPTER 1

### INTRODUCTION

Metals are not thought as an important optical instrument until the effect of the striking of a photon to a metal surface emerged in exactly same manner a rock toss into a pond. Metals have sea of quasi free electrons which are open to perturbations done by an oscillating electromagnetic field. Oscillation of electromagnetic wave induces oscillation of electrons well and the motion of the charges generates a radiation. The river of light set in motion on the surface of the metal is utilized beyond the scope of the ordinary transition of photons and electrons [1]. Historically, the charge river is thought to be similar to plasma so name of surface plasmon for the phenomenon is given by inspiration from the plasma at first [2]. Later it is seen that this phenomenon is not about the plasma. Since it always requires a medium and a whole story takes places on the surface it is called surface plasmon. It is quite understandable why the surface of the metal has a role in the story due to the distribution of electrons in a metal. Remind that –on suffix always refers to particle like property hence calls quantum mechanical approach. Similar to that photon is nothing but resonant mode of the vacuum, surface plasmons are the resonant modes of the oscillation mentioned. Even though plasmons are well known conceptually, the study of surface plasmon is accepted to begin with the interaction of the light and silver surface technically [3]. First encounter of surface plasmon in the literature is understood as the energy loss of electrons when interact with the metal [4]. Owing to many studies in the field of photonics and plasmonics the loss of energy effect is turned into gaining of intense energy. It is reported that light scattered from the surface is enhanced up to six orders of magnitude due to the surface plasmon effect[5]. Use of the surface plasmon propagation along the A A metal surface provides going beyond the diffraction limit in the applications of microscopy for imaging nanomaterials [6]. Propagation of plasmon along the

metallic surface which called surface plasmon polariton (SPP) opened new way of transmitting information faster than conventional electronics [7]. As structures of the metal are changed surface plasmon response to the metal is modified. To illustrate, surface plasmon polaritons can be guided along the metallic nano structures of photonic circuits [8], [9]. However, to obtain SPP requires phase matching such as using appropriate prism to couple or grating structure. Also, SPP may show bulk effect in detection. When the roughness of the metallic surface has nanoparticle like geometry, wavelength of the radiation would be comparable with the structure of the surface. Therefore, behavior of the electromagnetic wave in this boundary condition is expected to be different from planar dielectric/metal interface where SPP occurs. The electromagnetic modes are no longer continuous rather they are discrete valued which provides the localization of surface plasmons. That is localized surface plasmon (LSP) where the electric field enhancements are supposed to occur so called hot spots [10] [11]. Since the hot spots enhanced the electric field, they are vital for amplification of signal in spectroscopic measurements. They are used for the enhancement of the fluorescence signal and Raman scattering for surface enhanced Raman scattering (SERS) measurement [12],[13]. SERS is using the surface plasmon effect of metals and polarized molecules for the amplification of signal needed for identification of a molecule by Raman scattering [14]. Although Raman scattering process on which Raman spectroscopy grounds emits weak radiation, it is accepted as one of the most reliable identification techniques of molecules [15]. Therefore; it is crucial to increase the Raman signal to detect in spectroscopy. LSPs of the hot spots are needed at this point to increase the electric field locally then SERS would be available for the specific molecular detection. While LSP does not require a phase matching method, its difficulty lies behind the preparation of suitable substrate for emerging of hot spots and SERS measurement. Several techniques are employed for creating the roughness on the metallic surface which is capable of enhancing the field like a hot spot. nanolithography and etching the surfaces which are frequently used for the purpose are rather has their own difficulties to realize. A

very new technique of laser induced periodic surface structuring (LIPSS) can be utilized to generate the roughness of surface which may be available for the application of SERS [16]. LIPSS is introduced as partially uncontrollable surface damage done by ruby laser in 1965 [17]. For a long time, the topic remains untouched. Lately, lack of cost effective and reproducible technique to structure the material in nano scale revived the LIPSS as an efficient tool compared to traditional photolithography, electron beam lithography and others [18]. Despite the fact that no established theory explaining of every aspect of LIPSS is available [19], the control over the process via typical femtosecond laser parameters makes the LIPSS useful for many applications such as laser marking and coloring the metals [20] apart from the usefulness for the preparation of substrate for Raman scattering via SPP generating mechanism [21],[22]. Moreover, LIPSS is an universal event can be applied well to many substance. Thus, a metallic substrate after processed with LIPSS can be used directly or a dielectric can be coated by efficient metals after processed with LIPSS to see the Raman scattering in SERS. Therefore, LIPSS is expected to take an essential place in the measuring the SERS which is capable of detecting a single molecule [23].



## CHAPTER 2

### THEORETICAL FRAMEWORK

Plasmonics simply the study of the optical properties of noble metals, in particular gold and silver. Therefore; to understand plasmonics, light interaction with matter particularly metal should be considered at the first hand. When the metals are considered, free electrons on the surface responsible the major role in optical aspects of them. Then, the interface between a dielectric and a metal where is the surface plasmonic effect emerged. The optical aspect of the interaction of the electromagnetic wave with metal is hidden in the surface plasmon. All of them can be deduced from Maxwell equations and applying boundary conditions on the interface. Surface plasmons need a medium to propagate then suitable Maxwell equations for the propagation of the surface plasmon is similar to the propagation of the electromagnetic wave in medium.

$$\begin{aligned}\nabla \cdot \mathbf{D} &= \rho_{ext} \\ \nabla \cdot \mathbf{B} &= 0 \\ \nabla \times \mathbf{E} &= -\frac{\partial \mathbf{B}}{\partial t} \\ \nabla \times \mathbf{H} &= \mathbf{J} + \frac{\partial \mathbf{D}}{\partial t}\end{aligned}\tag{2.1} [24]$$

#### 2.1 Surface Plasmon Polariton and Plasma Frequency

Equation of motion of the electron on the metallic surface under an electric field can be written as

$$m \frac{dx^2}{dt^2} + m\gamma \frac{dx}{dt} + kx = e\mathbf{E} \quad (2.2)$$

Here second term represents the frictional damping and when the applied field is removed  $\gamma$  shows the rate of the decay of polarization hence has a unit [1/time]. Also, it can be represented in terms of polarization decay time  $\tau = 1/\gamma$ . The electric field changes harmonically when the electron intensity is low. In this paradigm it can be assumed that electrons mimic the electric field's movement then both of them position of the electron and electric field can be represented by harmonic functions  $\mathbf{E} = \mathbf{E}_0 e^{-i\omega t}$  and  $\mathbf{x} = \mathbf{x}_0 e^{-i\omega t}$  respectively.

Substituting this into equation (2.2)

$$(-m\omega^2 - im\omega\gamma + k)\mathbf{x} = e\mathbf{E} \quad (2.3)$$

solving for x and we know polarization is related to electric field by

$$\mathbf{P} = -Nex \quad (2.4)$$

we have

$$\mathbf{P} = \left( \frac{Ne}{-m\omega^2 - im\omega\gamma + k} \right) \mathbf{E} \quad (2.5)$$

shows that  $\mathbf{P}$  has strong frequency dependence in response to  $\mathbf{E}$ . if we arrange the equation in terms of resonant frequency which corresponds to simple harmonic oscillation

$$\omega_0 = \left( \frac{k}{m} \right)^{1/2} = 2\pi\nu_0 \quad (2.6)$$

it is obviously dependent on the particular material but incident electromagnetic wave. Resonant frequency refractive and absorptive properties related. Then

$$\mathbf{P} = \left( \frac{\frac{Ne}{m}}{-\omega^2 - i\omega\gamma + \omega_0^2} \right) \mathbf{E} \quad (2.7)$$

Therefore if there is resonant effect of the material electrons can be excited easily or perturbed at this resonant frequency of the material[25], [26]. It is obvious from the equation when  $\omega = \omega_0$ ,  $P$  has the greatest value. When  $\omega_0 = 0$  it is unbounded electrons which are on the surface a metal.

$$\mathbf{D} = \varepsilon_0 \mathbf{E} + \mathbf{P} \quad (2.8)$$

Leads

$$\mathbf{D} = \varepsilon_0 \left( 1 - \frac{\omega_p^2}{\omega^2 + i\gamma\omega} \right) \mathbf{E} \quad (2.9)$$

Where  $\omega_p = \frac{ne^2}{\varepsilon_0 m}$  is the plasma frequency of quasi free electrons on the surface.

Then dielectric function of the metal can be obtained as

$$\boldsymbol{\varepsilon}(\omega) = 1 - \frac{\omega_p^2}{\omega^2 + i\gamma\omega} \quad (2.10)$$

which obviously have real and imaginary parts. If we separate those parts individually we take

$$\boldsymbol{\varepsilon}_1(\omega) = 1 - \frac{\omega_p^2 \tau^2}{1 + \omega^2 \tau^2} \quad (2.11)$$

$$\boldsymbol{\varepsilon}_2(\omega) = \frac{\omega_p^2 \tau^2}{\omega(1 + \omega^2 \tau^2)}$$

For  $\boldsymbol{\varepsilon}(\omega) = \boldsymbol{\varepsilon}_1(\omega) + i\boldsymbol{\varepsilon}_2(\omega)$  in terms of  $\gamma = \frac{1}{\tau}$ .

When  $\omega < \omega_p$  metals show their metallic properties such as reflectivity. When  $\omega$  is closer to  $\omega_p$  dielectric function approaches real part. But in the case of noble metals such as gold and silver which are important for the surface plasmon, the situation is changed by interband transmission. When the frequency is very low  $\omega < \tau^{-1}$

absorptive properties is revealed by making real and imaginary part of the refractive index  $\eta = n + i\kappa$  close to each other.

$$n \approx \kappa = \sqrt{\frac{\varepsilon_2}{2}} = \sqrt{\frac{\tau\omega_p^2}{2\omega}}$$

Gives the absorption coefficient

$$\alpha = \left(\frac{2\omega_p^2\tau}{c^2}\right)^{1/2} \quad (2.12)$$

According to Beer's Law of absorption electromagnetic wave propagates through metal with skin depth  $\delta = 2/\alpha$  which is a very important parameter in the aspect of surface plasmon polariton [26].

### 2.1.1 Condition for Excitation of the Surface Plasmon Polariton

Let consider transverse electric wave comes to the interface between a dielectric which has dielectric constant  $\varepsilon_d$  and a metal  $\varepsilon_m$  which has a dielectric function as it is illustrated in *Figure 2.1*.

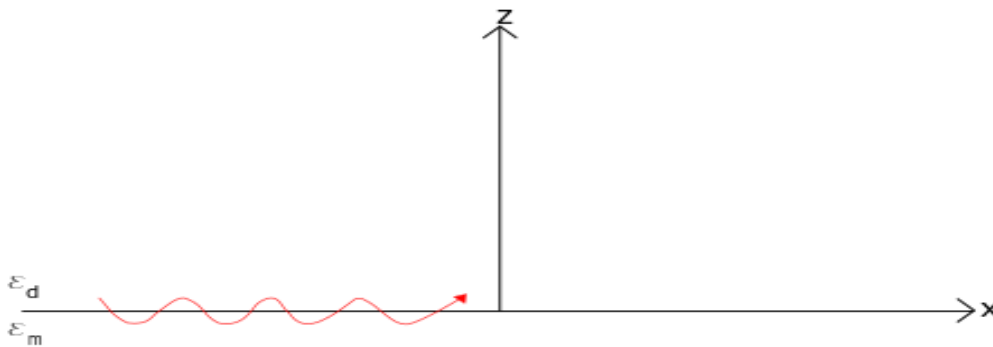


*Figure 2.1. The surface plasmon polariton on the interface between a dielectric and a metal surface is similar to electromagnetic wave propagation on boundary*

For  $z > 0$  in air

$$E_1 = E_{1y} e^{i(k_x x - \omega t)} e^{-\alpha_1 z} \quad \alpha_1 > 0 \quad (2.12)$$

For  $z < 0$ ,

$$E_2 = E_{2y} e^{i(k_x x - \omega t)} e^{-\alpha_2 z} \quad \alpha_2 > 0 \quad (2.13)$$

We know from Maxwell equations that  $\nabla \times \mathbf{E} = -\mu_0 \frac{\partial \mathbf{H}}{\partial t}$  and derivative of the harmonic part in space and time is  $\frac{\partial}{\partial t} = -i\omega$ . Then, according to curl product

$$H_x = -\frac{1}{\mu_0 i \omega} \frac{\partial E_y}{\partial z}$$

and

$$H_z = -\frac{1}{\mu_0 i \omega} \frac{\partial E_y}{\partial x}$$

Full magnetic equations are

$$z > 0, H_1 = \frac{1}{\mu_0 i \omega} [\alpha_1 \hat{x} + i k_x \hat{z}] E_1 e^{i(k_x x - \omega t)} e^{-\alpha_1 z} \quad (2.14)$$

$$z < 0, H_2 = \frac{1}{\mu_0 i \omega} [-\alpha_1 \hat{x} + i k_x \hat{z}] E_2 e^{i(k_x x - \omega t)} e^{\alpha_2 z} \quad (2.15)$$

Applying boundary conditions at the boundary  $z = 0$ ,  $H_{\parallel}$  should be continuous imply that  $\alpha_1 \hat{x} = \alpha_2 \hat{x}$  but this is not the case therefore surface plasmon cannot exist in TE mode.

Let's look at the transverse magnetic mode

For  $z > 0$  in air

$$H_1 = H_{1y} e^{i(k_x z - \omega t)} e^{-\alpha_1 z}, \alpha_1 > 0 \quad (2.16)$$

For  $z < 0$

$$H_2 = H_{2y} e^{i(k_x z - \omega t)} e^{-\alpha_2 z}, \alpha_2 > 0 \quad (2.17)$$

We know from Maxwell equations that

$$\nabla \times \mathbf{E} = -\varepsilon_0 \frac{\partial E}{\partial t} = -i\omega\varepsilon E \quad (2.18)$$

$$E_x = -\frac{1}{\varepsilon i\omega} \frac{\partial H_y}{\partial z} \text{ and } H_z = -\frac{1}{\varepsilon i\omega} \frac{\partial H_y}{\partial x} \quad (2.19)$$

$$z > 0, E_1 = \frac{1}{\varepsilon_d i\omega} [-\alpha_1 \hat{x} + ik_x \hat{z}] H_1 e^{i(k_x x - \omega t)} e^{-\alpha_1 z} \quad (2.20)$$

$$z < 0, E_2 = \frac{1}{\varepsilon_m i\omega} [-\alpha_2 \hat{x} + ik_x \hat{z}] H_2 e^{i(k_x x - \omega t)} e^{-\alpha_2 z} \quad (2.21)$$

at the boundary  $H_{\parallel}$  is continuous  $H_1 = H_2$  and  $E_{\parallel}$  implies that if  $\frac{-\alpha_1}{\varepsilon_d} = \frac{\alpha_2}{\varepsilon_m}$  dispersion says that  $\varepsilon$  can be negative.

Then either  $\varepsilon_d$  or  $\varepsilon_m$  should be smaller than zero. It is valid.

$$\alpha^2 - k_x^2 = \frac{\omega^2}{c^2} \varepsilon_r \mu_r \quad (2.22)$$

$$z > 0, \alpha_1^2 - k_x^2 = \frac{\omega^2}{c^2} \varepsilon_1 \mu_1 \quad (2.23)$$

$$z < 0, \alpha_2^2 - k_x^2 = \frac{\omega^2}{c^2} \varepsilon_2 \mu_2 \quad (2.24)$$

together gives

$$\frac{\alpha_1^2}{\alpha_2^2} = \frac{1}{c^2} \frac{\omega^2 \varepsilon_1 \mu_1 + k_x^2 c^2}{\omega^2 \varepsilon_1 \mu_2 + k_x^2 c^2} \quad (2.25)$$

remember  $\frac{\varepsilon_1}{\varepsilon_2} = \frac{-\alpha_1}{\alpha_2}$  substitute into the equation we obtain dispersion relation for

surface plasmon  $k_x = \frac{\omega}{c} \sqrt{\frac{\varepsilon_1 \varepsilon_2}{\varepsilon_1 + \varepsilon_2}}$  when  $\varepsilon_1 = -\varepsilon_2$  and  $k_x \rightarrow \infty$  gives  $\lambda \rightarrow 0$  [24].

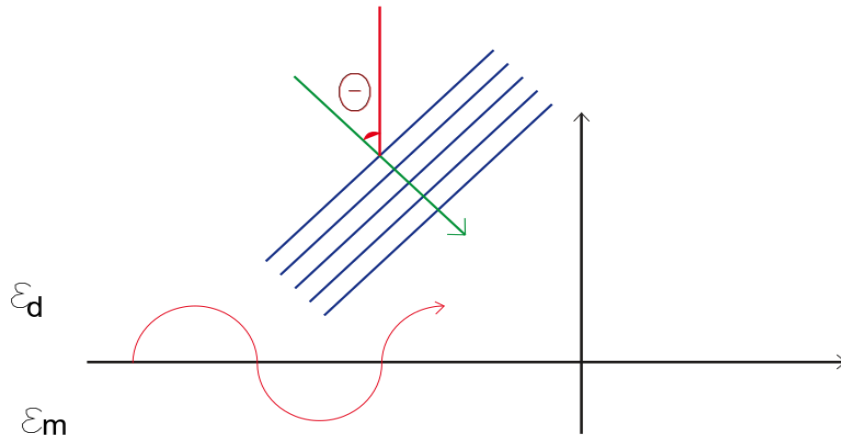


Figure 2.2 Plane wave interaction with metal surface

### 2.1.2 Phase- Matching

Having the propagation constant  $k_x$  is greater than the wave vector of the light in the dielectric side evanescent decay occurs on both metal and dielectric surfaces and wave is confined. Then excitation of SPP cannot be achieved. It requires some techniques such as phase- matching. Then two-dimensional wave propagation takes place at the interface between these media which is surface plasmon polariton SPP. But SPP cannot be excited without a proper phase matching such as grating or prism coupling. The effect of the process is to provide enough momentum for SPP to propagate [27].

### 2.2 Localized SP

When the size of the boundaries is comparable with the wavelength, electromagnetic modes have discrete values depending on the  $\omega$ . The name of the localized surface plasmon LSP of the modes origins from that discrete nature mentioned. That nature of the electromagnetic modes does not relate to  $k$  anymore. Since propagation property of the modes is lost [26]. These type of excitation does

not require setting like a phase matching instead they naturally occur by scattering from sub-wavelength metal nanoparticles. Moreover, curvature of the surface of the nanoparticles generates an effective restoring force on the electrons so that resonance can arise. As a result the field amplification is achieved in both the near field zone and inside the particle [27].

While Localized Plasmon does not need to be employed by phase matching methods, it occurs only when certain nanostructures achieved. For example, nanoparticles on the metal surface when the size of the particle  $d$  is smaller than the incident wave length  $d \ll \lambda$  can be a substrate for the localized surface plasmon. So it highly depends on the geometry and the size of the nanostructures on the metal surface [28]. Having smaller particles unlike the planar surfaces as in the case of SPP provides an approximation to analyze the physics of the excitation LSP. When the particle is small electromagnetic oscillation can be considered as static over a particle and simple undergraduate problem of metal sphere inside an electrostatic medium can be applied well to the excitation of localized surface plasmon. This is called quasi-static approximation. After the field is calculated, time dependence of harmonic oscillator can be simply added to predict the resonant field enhancement [27].

$$\mathbf{p} = 4\pi\epsilon_0\epsilon_m a^3 \frac{\epsilon - \epsilon_m}{\epsilon + 2\epsilon_m} \mathbf{E}_0 \quad (2.26)$$

where  $a$  is the radius of the sphere.

Therefore, it is seen that electric field induce a polarization inside the sphere and the polarization is proportional to  $\mathbf{E}_0$ . Remembering

$$\mathbf{p} = \epsilon_0\epsilon_m \alpha \mathbf{E}_0 \quad (2.27)$$

Then we obtain polarizability of small sphere

$$\alpha = 4\pi a^3 \frac{\epsilon - \epsilon_m}{\epsilon + 2\epsilon_m}. \quad (2.28)$$

when  $|\varepsilon + 2\varepsilon_m|$  is minimum we get the resonant enhancement. Near the resonance the dipole surface plasmon condition is valid.

$$\text{Re}[\varepsilon(\omega)] = -2\varepsilon_m \quad (2.29)$$

It shows that resonance frequency highly depends on the dielectric. Increase in  $\varepsilon_m$  generates the red shift in the resonance. Thus, the resonant enhancement of metallic nanostructures can be used to detect the change in refractive index [27].

Unlike SPP, to obtain LSP is not challenging since it does not require certain settings such as phase matching. Main difficulty of the LSP observation is the preparation of a suitable substrate which provides discrete electromagnetic modes by its comparable size of the structure with the incident wavelength. It is known that rough metal structures are beneficial to increase Raman scattering signal and resonant Raman scattering signal [5], [3], [12]. Interaction of electromagnetic waves with the metal nanoparticles on rough surface can create zones where the electric field intensity is high. These zones are called hot spots [29],[28], [11]. The field in the hot spot can be used to detect SERS signal sometimes with the nonlinear effect [30], [31], [32]. Intuitively, the electric field in the hot spot can be considered as being trapped. When light incidence to the rough surface, it is scattered between these random nanostructured planes that are formed by the roughness of the surface and the intensity between these planes is higher than the other zones on the substrate[29]. Obviously, the energy of hot spots where the electric field intensity is high is larger than the other zones without hot spots. Only the distribution of the energy on the substrate is changed then total energy is conserved.

### **2.3 Laser Induced Periodic Surface Structures**

A few techniques are used for realizing the hot spots such as using metal nanoparticles via solution and nanolithography and evaporation on a substrate [29]. Laser induced periodic surface structure (LIPSS) is expected to overcome the

difficulty in designing a substrate that forms the hot spots. LIPSS can be utilized for generating rough structures so that the increase of the signal of SERS by the enhancement of the field nears the rough surfaces [33], [16]. LIPSS is compatible with dielectrics, semiconductors and metals. Moreover, nanostructures are achieved in a simple cost-effective process in LIPSS which does not require vacuum environment or chemical treatments. To see the field enhancement effect, it can be applied over silver or it can be applied over dielectric at first then coated with appropriate metals [16],[34]. During the formation of LIPSS several mechanisms can take place as a result there is no general theory of the formation has been established that covers each aspect of the LIPSS [19]. Before the process has been given the name, LIPSS are thought simply damaging of lasers to the surfaces and scattering of laser light at scratches of the surface. This explanation provided to consider some parameters that are still useful for explaining LIPSS [35]. Main parameters to generate controlled surface morphology are simply the laser fluence and pulse number and repetition rate of laser. Fluence is related power via [25]

$$\text{Laser Fluence}[\text{J}/\text{cm}^2] = \frac{\text{Power} [\text{W}]}{\text{Repetition Rate} [\text{Hz}] \times \text{Spot Area}[\text{m}^2]} \quad (2.30)$$

Later formation of it is linked to surface polariton along the irradiance on the surface [36]. Then the efficacy factor theory is proposed by Sipe and affirmed experimentally for some substances. According the theory, laser radiation is not absorbed equally over the surface due to roughness of the surface and with the help of the efficacy factor  $\eta$ , k wave vector of LIPSS can be found in terms of laser parameters. Therefore, shallow grooves done by LIPSS are able to be explained in the paradigm of the theory of surface- scattered electromagnetic waves (SEW). But deep grooves and other texture formation need more complex proposals such as the SPP excitation [37]. All of these approaches explained some events of LIPSS successfully. But some phenomenon such as feedback mechanism is still unexplainable under this point of light. Even efficacy theory which is in good agreement with many aspects of the LIPSS process is not enough to establish full

theory of formation of LIPSS. Rather, explanations which are in good agreement with particular types of LIPSS are suggested. Thus, LIPSS formation can be divided into two main sections which are low spatial frequency LIPSS (LSFL) and high spatial frequency LIPSS (HSFL). The division is based on their periods compared to the irradiance wavelength. When the period is much smaller than the wavelength, typically  $\Lambda_{HSFL} < \lambda/2$ , LIPSS are thought to be formed self-assembly and this corresponds HSFL or they are called nanoripples. If the period of LIPSS is close to the irradiance wavelength  $\lambda/2 \leq \Lambda_{LSFL} \leq \lambda$  under the normal incidence with respect to the polarization of laser beam [19]. LIPSS are generated via femtosecond laser and the period should be considered with laser parameters and corresponding regime. Which mechanisms play role in the formation of HSFL is not obvious. Some types of them are accepted self-organized. Generally, it is known that superficial oxidation takes place in the formation of HSFL in metal surfaces such as titanium [38] or nickel [39]. Structures formed by SEW and excitation of surface plasmon polaritons are generally seen on efficiently absorbing materials under perpendicular laser beam to the LIPSS structure. This structure results in periods in LSFL regime and SPP periods can be taken as  $\Lambda_{LSFL} = \Lambda_{SPP} = \lambda \times Re \left\{ [(\varepsilon + 1)\varepsilon]^{1/2} \right\}$  where  $\varepsilon$  is the bulk dielectric permittivity [40], [41]. It is expected that the surface formation by the excitation of surface plasmon polariton is useful for SERS [21].

## 2.4 Surface Enhanced Raman Scattering

SERS is simply a spectroscopic technique that enhances the field of localized surface plasmons for the use of Raman scattering. Therefore; it is related to Raman and surface plasmon. As is evident from its name, it is the process that takes places on the surface of the substrate. And, molecules should be adsorbed on the surface of the metals. Next, enhancement is needed to observe the signal of SERS which is obtained by the interaction of electromagnetic waves with the nanostructures of the metal, namely by hot spots or localized surface plasmons as it is mentioned

previously. Also, S in SERS refers to scattering if optical aspect is matter or spectroscopy if it is about the analysis of measurement. Since SERS measures the signal of Raman scattering of probes, one needs to look at Raman scattering to understand the SERS better [26].

### 2.4.1 Raman Scattering

Scattering means absorption of a photon while emitting another one. If the emitted namely scattered photon and the incident one has the same energy but probably having different polarization or direction, it is called elastic scattering. By the way, if process involves a molecule it is named Rayleigh scattering. On the contrary, if they have different energy depending on the transition of electron, it is called inelastic scattering. A molecule having inelastic scattering in which a vibrational or a rotational transition exists, it is mainly Raman scattering. Better understanding might be possible with the illustration of Jablonski diagram in terms of quantum mechanics.

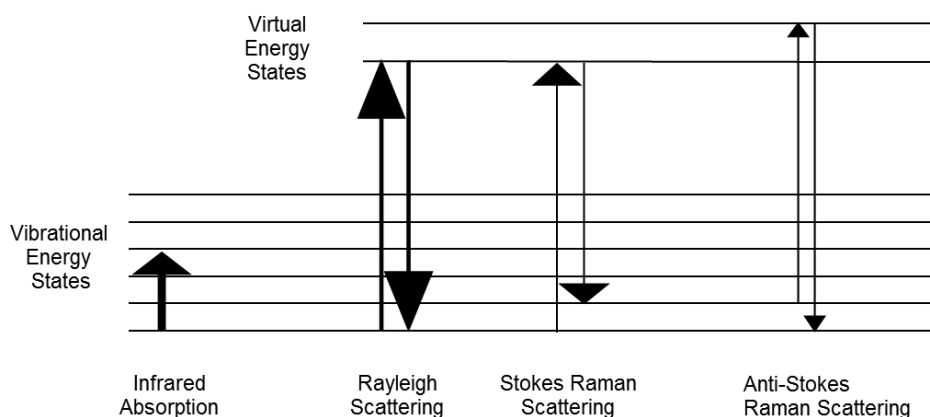


*Figure 2.3 Jablonski Diagram*

Apart from other scattering, in Raman scattering energy of the incident wave does not have to match with the transition energy between the corresponding two electronic states. Even, Raman scattering can take place when there is no

absorption of a molecule. It depends only on the vibrational or rotational states of the molecule. It is appreciated well in quantum mechanical point of view. A molecule in an excited state can be considered as in virtual state which is not one of a real electronic state of the molecule. That is a virtual state is just a model to visualize the absorption and scattering process. When incident wave perturbs the molecule, it can be thought that it goes down another state from the virtual state. Then, the emitted photon has energy different from incident one by

$$\frac{h}{2\pi} \omega_\nu = E_L - E_S$$

This process is called Stokes. There is also another one which is called anti-stokes. It might happen that virtual state of the molecule has the same energy with an electronic state of the molecule. In the aligned system of the states, the absorption is realized and resonant effect is emerged. It is called resonance Raman scattering (RRS) which has higher efficiency than the Raman scattering. It is expected that stokes scattering is stronger than the anti-stokes one. For stokes includes transition from ground state at which more particles exist. Even though increasing temperature increase the anti-stokes effect, stokes is still main scattering process.

For Rayleigh scattering, an electric field in the vicinity of a molecule induces a polarization in the molecule as in the classical electromagnetic theory. Oscillating electric field is

$$\mathbf{E} = \mathbf{E}_0 \sin\omega t$$

where  $\omega = 2\pi\nu$ ,  $\nu$  is the frequency of the incident wave and  $\mathbf{E}_0$  is the amplitude of the electric field wave.

The dipole moment of the polarization is simply given as

$$\mathbf{p} = \alpha \mathbf{E}$$

where  $\alpha$  is the polarizability.

Then,

$$\mathbf{p} = \alpha \mathbf{E}_0 \sin 2\pi\nu t$$

It is seen that dipole radiation has the same frequency with the incident light's frequency. It is assumed that oscillation is small. Then Taylor expansion is available for the polarizability  $\alpha$

$$\alpha = \alpha_0 + \frac{\partial \alpha}{\partial x} x \quad (2.29)$$

where  $x$  is the position of the molecule and it is assumed oscillates with the electric field  $x = x_0 \sin 2\pi v_m t$ ,  $v_m$  is the molecular frequency.

With this polarizability is

$$\alpha = \alpha_0 + \frac{\partial \alpha}{\partial x} x_0 \sin 2\pi v_m t \quad (2.30)$$

and dipole moment is

$$\mathbf{p} = \alpha_0 \mathbf{E}_0 \sin(2\pi v t) + \frac{\partial \alpha}{\partial x} x_0 \mathbf{E}_0 \sin(2\pi v_m t) \sin(2\pi v t) \quad (2.31)$$

Then with the use of trigonometric relation

$$\mathbf{p} = \alpha_0 \mathbf{E}_0 \sin(2\pi v t) + \frac{1}{2} \frac{\partial \alpha}{\partial x} x_0 \mathbf{E}_0 [\cos 2\pi(v - v_m) t - \cos 2\pi(v + v_m) t] \quad (2.32)$$

Here it is seen that there is a stronger band of incident frequency and there are symmetrical frequency bands around the incident frequency which are weaker in Raman spectrum of the vibrating molecule. Moreover, it is concluded that if  $\frac{\partial \alpha}{\partial x} = 0$  molecule is Raman inactive. Also, apparently Raman scattering has weak signal so it requires amplification technique to be used effectively. One of them is SERS.

#### 2.4.2 Enhancement Factor

Enhancement by SERS is based on the two factors which are electromagnetic and chemical enhancements. Latter consists of chemical bonding of probes.

Electromagnetic enhancement is mainly responsible the enhancement of SERS. Hence, explanation of electromagnetic origin of Raman scattering is applicable well into the concept of electromagnetic enhancement of SERS.

Regarding the use of metal in SERS, Raman scattering should be reconsidered with localized surface plasmon effect. Next, rearrangement of the dipole moment of Raman  $p$  and the polarizability  $\alpha$  in accordance with use of a rough metal surface are supposed to be result in radiation enhancement. This requires analyzing the electromagnetic consideration for a particular geometry at hand and relating the solution with the SERS counterparts. Electric field felt by the molecule  $E_{Loc}$  is different from incident electric field  $E_{Inc}$  in the aspect of magnitude and orientation. The hot spot on the surface is where the increase in  $E_{Loc}$  with respect to  $E_{Inc}$  occurs and SERS signal is caught.  $E_{Loc}$  induces polarization and Raman dipole here is  $\mathbf{p} = \alpha \mathbf{E}_{Loc}(\omega)$  energy of the dipole is proportional to square of the electric field then enhancement in the point is the nothing but the ratio of square of the localized field to the square of the incident field

$$M(\omega) = \frac{|E_{Loc}(\omega)|^2}{|E_{Inc}|^2} \quad (2.33)$$

$M(\omega)$  is the local field enhancement factor.

Like the field, radiation dipole is also affected by the metal. Since environment is crucial for the emission power of the oscillation of the radiation dipole, total power radiated can be taken account for enhancement factor.

$$M(\omega) = \frac{P_{Rad}}{P_0} \cdot P_0 \quad (2.34)$$

is the power in the free space. In terms of enhanced intensity ( $I_{SERS}$ ), number of enhanced molecule ( $N_{SERS}$ ), Raman molecule ( $N_{Raman}$ ) and intensity of Raman ( $I_{Raman}$ )

$$EF = \frac{I_{SERS}}{N_{SERS}} \times \frac{N_{Raman}}{I_{Raman}} \quad (2.35)$$

It is natural to ask whether energy is conserved when power is enhanced in some locations. Energy conservation is still valid as source of external energy does not change during the process. The way of radiation of power is altered by  $\frac{dP_{Rad}}{d\Omega}$  radiation of power in the far field per solid angle in a certain direction. To illustrate, when the dipole radiation is in close proximity of a perfect reflector is totally reflected and no power radiation emerges.

## CHAPTER 3

### EXPERIMENTAL METHODS

#### 3.1 Preparation of Substrates

The experiment requires a few layered substrates. As a lowest layer silicon wafer with the properties such that p-type, boron doped, having resistivity of 5-10  $\Omega$ .cm, Czochralski, <100>, single side polished is used. A thin film of molybdenum, titanium or nickel is coated over the silicon layer. Later, this layer is processed with laser. And crystal violet (CV) dyed over silver layer which is placed on that metallic layer to observe the effect of SERS. Cross sectional view of the whole configuration of the layers look like in the Figure 3.1.

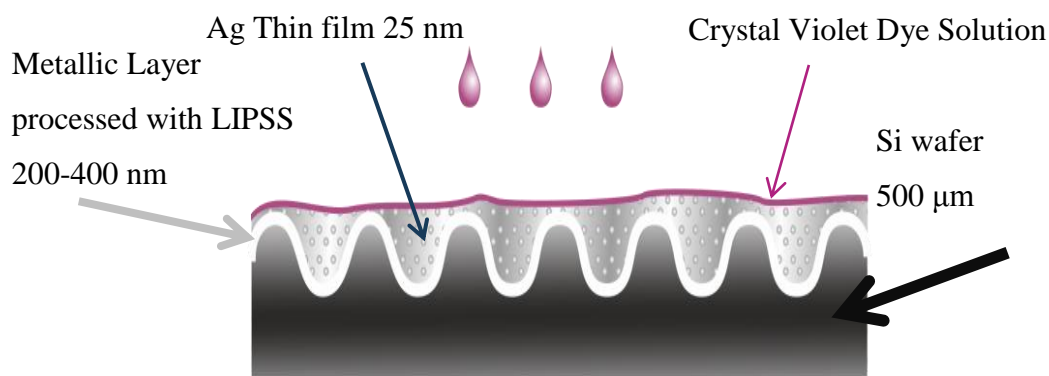


Figure 3.1 Configuration of the layers of the SERS substrate

Not only thin films of the mentioned elements but also plate of titanium and nickel which are coated by silver and dyed with CV is used for comparing the differences between thin film and bulk of the element and thickness matter. Additionally, titanium coated glass is used in the experiment as well. Schematic representation of

the general preparation steps of the substrates can be seen on the diagram below. As a common practice of cleaning of silicon wafers, Hydrofluoric acid (HF), RCAI or piranha, and RCAII cleaning procedures are applied respectively. The first step is used for removing oxide layer from surface of the silicon wafer, RCAI cleaning provides to eliminate organic residues. The second step is required for removing the inorganic residues like metal contamination. Samples are awaited in each solution per 15 minutes.

After the cleaning procedure, wafer is ready for coating of metallic thin layer of Ti, Ni or Mo by various evaporation techniques. Ti and Mo thin films are generated by exposing Si wafer to Argon gas at 5 mTorr for a required time up to desired thickness typically more than an hour in rf sputter (Nanovak NVTH-460T). The Wafer is left in rf sputter in 100 W for Ti coating and in 75 W for Mo coating. Ni is coated via e-beam evaporation in 3mA emission current and 1.1 rate. Thickness values read from thickness monitors is checked by measurement via Dektak. The substrates obtained according to their thickness are shown in the table.

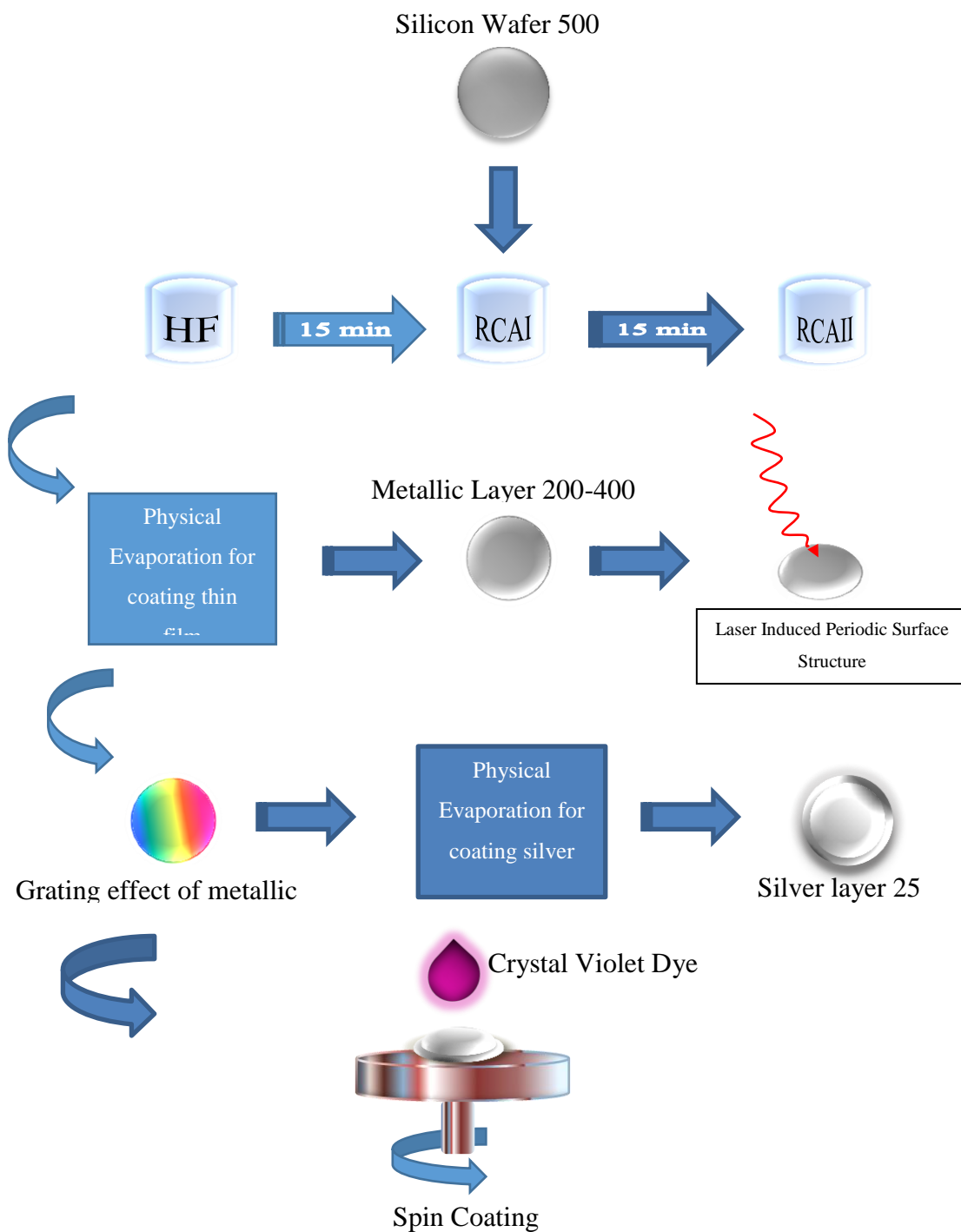


Figure 3.2 Steps involved in the preparation of SERS substrate

Table 3-1 Thickness and type of the metallic interlayer of the SERS substrate

Ti on glass	-	300	-	
Ti	400	300	200	280 $\mu$ m bulk
Mo	400	-	-	
Mo on Ti	-	-	200	
Ni	-	300	-	500 $\mu$ m bulk

Plate of metals are polished to observe the surface effects easier. After obtained thin films Laser induced surface structure (LIPSS) is applied to them to rough their surface which is required to observe the localized surface plasmon effect. Once the roughness in the surface is provided, it is ready for coating of silver (Ag) via thermal evaporation (Nanovak NVTH-460T). For 25 nm coating of Ag, 100 W power and 0.8 rate speed of coating is used for 10 minutes. And finally, substrates are ready for SERS after the applying dye via spin coating (Specialty Coating Systems Spincoat G3-8) in 2000 rpm for 30 seconds with 5 s of acceleration and 3 s of deceleration time. Dye molecule is  $10^{-4}$ crystal violet (CV) which is used typically to observe the Raman scattering. Adsorption of CV molecules to the metallic surface.

### 3.2 Laser Induced Periodic Surface Structure Formation

LIPSS is formed via laser system which has pulse width 310 fs, and a central wavelength of 1032 nm and a repetition rate of 1MHz. The spot size of the beam on the surface of the metal is about 10  $\mu$ m. Experiment is done in air. Polarizer and a half wave plate combination is used for controlling the power and polarization. Laser beam generally is set to have horizontal polarization during the experiment which is perpendicular to scanning direction. There is a loss of power in the system such that power obtained after focusing is about 40% of the power before focusing.

LIPSS formation is done in ablation regime. The pattern on the surface due to the formation of LIPSS is obtained by depending on not only material properties like dielectric function of the material but also the scanning parameters such as laser fluence, scanning speed, polarization. Laser fluence is proportional to power which can be read simply via power meter with the relation (2.30). Ti is in the form of a bulk, thin film on the glass, thin film on the Si, Mo on the Si and on very thin Ti layer, Ni coated on the Si in different thicknesses are used as a substrate for the LIPSS.  $0^\circ$  and  $50^\circ$  angle of the half wave plate is set vertical polarization and horizontal polarization with respect to scanning direction. 5x5 mm squares are processed at different scan speed between 20 and 3000 mm/s and at different average power values between 300 and 900 mW depending on the sample requirement. All parameters are designed for the particular material to be processed by laser regarding their physical structure, thickness, the dielectric function, and ablation threshold while hatch distance is kept constant about  $4.5\mu\text{m}$ . For example, while some surface changes appear on Si surface between the average power 680-780 mW and scanning speed 1000- 1400mm/s for single pulse, Ti and Mo are able to be textured in lower power and according speeds. Although they are all can be structured with higher power, other effects of high power can generate some unwanted results. Ni is exceptionally studied with lower speed values.

After all samples are processed with these parameters as another part of LIPSS Ti is processed with firstly at  $0^\circ$  angle of vertical polarization immediately after polarization is changed to horizontal and the second process is done in the same area of the sample. During the experiment grating is observed well. Figure 3.4

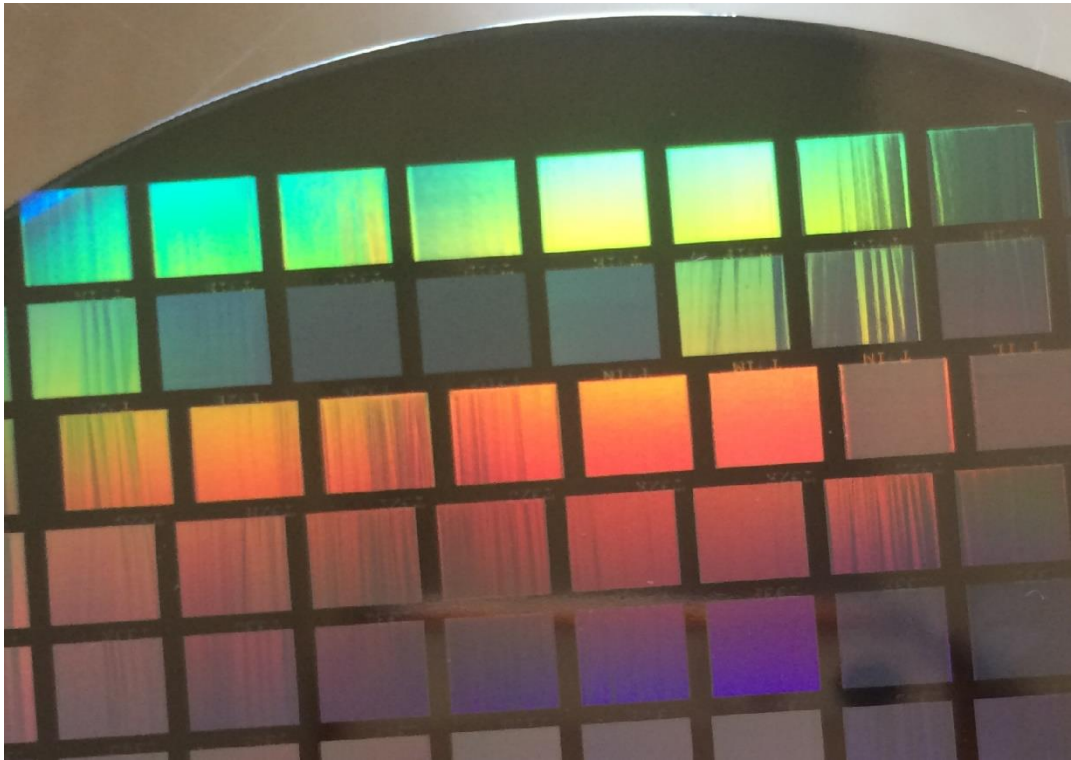


*Figure 3.3 Gratings by LIPSS on the 200 nm thicken titanium surface*

### **3.3 SEM as An Analysis Tools**

We benefited from Scanning Electron Microscope, angle resolved scattering and Raman spectroscopy in order to observe grating and hot spot effect for the electric field enhancement. All substrates were subjected to Scanning Electron Microscope (SEM) (ZEISS EVO HD15) operating at 20 kV. The images of substrates processed with LIPSS are taken with 5kX, 10kX, 20kX and 50kX magnifications. Also, SEM images are processed for period analysis and the size of the emerged structures.

### 3.4 Angle Resolved Scattering

The device, which has two concentric rotation stages, has a screen with a 3mm (or 6 mm) aperture to control the angle of incidence. A fixed path laser beam with a wavelength of 532 nm and 1.5 mm full width half maximum Gaussian profile passes through the aperture center modulated with the optical chopper. In the second stage, the detector arm is controlled, which rotates around the center. The scattered/diffracted signals in the reflection are scanned by this detector.

Diffused light is combined with a large core fiber from a 3mm diameter diffuser film at a distance of 244mm from the center opening; this corresponds to the approximate planes of  $1.2 \times 10^{-4}$  steradians or aperture that collects a light of  $0.7^\circ$  around the plane of rotation on the detector arm. This small collector area provides very little inhibition of the light coming around the incidence light in reflection measurements (less than  $2^\circ$ ), while it is sufficient to collect almost all laser beam power directly incident to the collector (in transmission mode). Corresponding to  $s = 1.2 \times 10^{-4}$  steradians, or  $0.7^\circ$  around the plane of rotation, a diffuse light is attached to a large core optical fiber from a 3mm diameter diffuser film at a distance of 244 mm from the center opening. While all laser beam power can be collected enough when it comes directly to the collector (in transmission mode), the small collector area creates part of blocking in the reflection light of the incidence light. A group of screens are exploited for stray light reduction. Using a lock-in amplifier, the signal measurement is variable and the other side of the fiber is combined with the variable gain silicon photodetector.

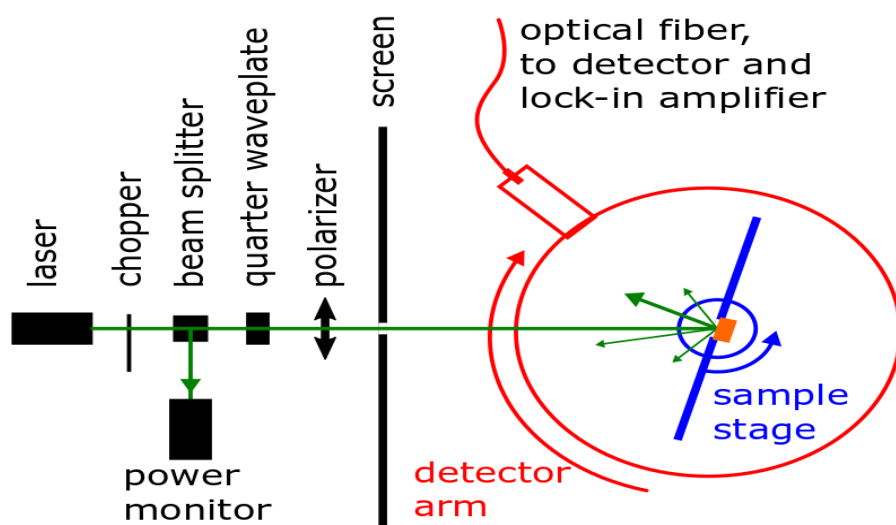
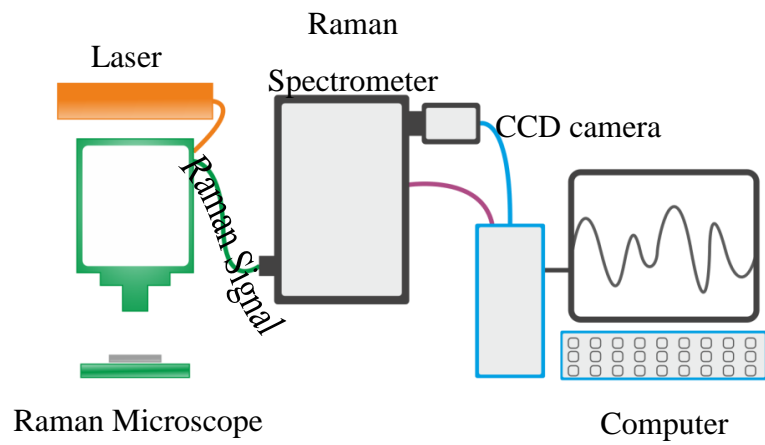


Figure 3.4 Experimental Configuration of Angular Resolved Scattering

### 3.5 Raman Measurement

As is seen from the Figure 3.5, which represents the experimental set up of Raman measurements, a 532 nm radiation with frequency doubled DPSS Nd-YAG SLM laser (Laser Quantum torus) at power of 0.2 mW is coupled to an optical fiber cable to transfer light through which our sample was illuminated with the help of an illumination source inside the Raman head. By doing so, there was a 17  $\mu\text{m}$  diameter focal spot size with the help of 100X objective lens. In the mechanism of the Raman head, there is an exhaust port which helps to filter Rayleigh scattered photons. Moreover, in order to keep CCD camera safe, shorter than 532 nm wavelengths were filtered as well. In the meantime, Raman head collected inelastically scattered photons and sent them to the spectrometer through another optical fiber cable. The collected light was analyzed by Raman spectrometer (Horiba Jobin-Yvon iHR550) with a 1024x256 pixel CCD (Horiba Synapse). The acquisitions were performed with 98  $\mu\text{m}$  slit width and 600 grooves/mm blazed grating at 500 nm. As a final step, CCD camera sent the raw data to the computer and these data were analyzed by using Andor software.



*Figure 3.5 Raman Spectroscopy Set up for the measurement of SERS*



## CHAPTER 4

### RESULTS AND DISCUSSION

#### 4.1 SEM Images of LIPSS

Ripples and grooves are generated on metals and semiconductor Si surfaces by linearly polarized laser. It is understood that transferred energy by the laser light generates the heat accumulation to the surfaces.

Observed structures formed perpendicular to the laser polarization and have periods about 900 nm which close the wavelength. It is agreement with the fact that metals are formed structures of having period close the irradiation wavelength in the mentioned conditions. That is low spatial frequency LIPSS LSFL is observed [42], [43]. Although it is thought that the formation is related to scattering of electromagnetic wave (SEW) model of LIPSS partially according to Sipe [37], the excitation of SPP is the responsible mechanism as it is suggested in [44]. For 400 nm thick Ti surface and 700 mW power it is observed that when the scanning speed is higher, respectively larger periods is obtained, But to correlate the scanning speed and the period more investigation is needed. Some of the forms obtained are shown in the Figure 4.1

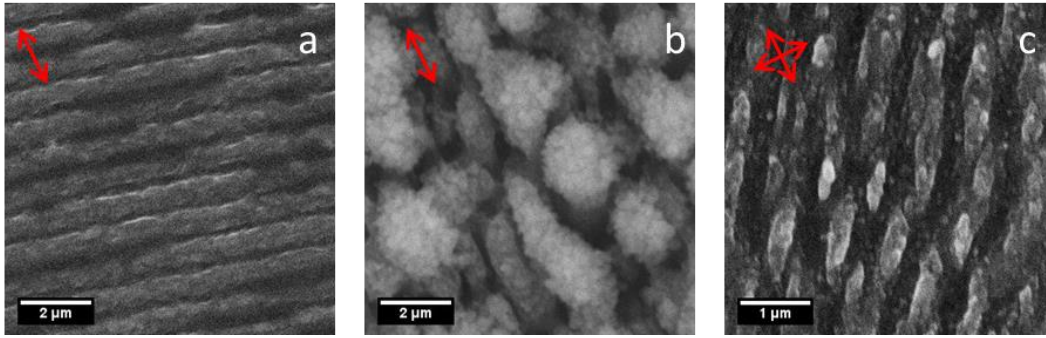


Figure 4.1 Some forms obtained in a and c perpendicular polarization is used in b both perpendicular and parallel polarization are used successively. Texture in a and b is formed on Ti in c it is Mo surface.

Number of pulses per spot is inversely proportional to scanning speed in agreement with the equation of number of pulses per spot

$$pps = \frac{w \cdot f}{v} \quad (4.1)$$

where  $w$  is the Gaussian width of the laser beam and  $f$  is the repetition rate, and  $v$  is the scanning speed. Scanning speed and period relation exhibit the SP excitation mechanism according to many studies [45][46][47]. When the speed is slower more overlapping as a result more ablation occurs. In the Si case, as a semiconductor Si is not expected to be involved in SPP excitation mechanism. But during the process Si changes its optical properties and reveal metallic behaviors[48]. More overlapping generates more thermal effect on the infected area.

LSFL requires to be processed in this regime, otherwise different kind of structures might emerge. Also polarization affects the structures. Interestingly, successive application of different polarization results in different textures.. When different polarization is applied successively lower periodic structures can be seen with the 2D grating structures Figure 4.1b.

## 4.2 Angle Resolved Scattering

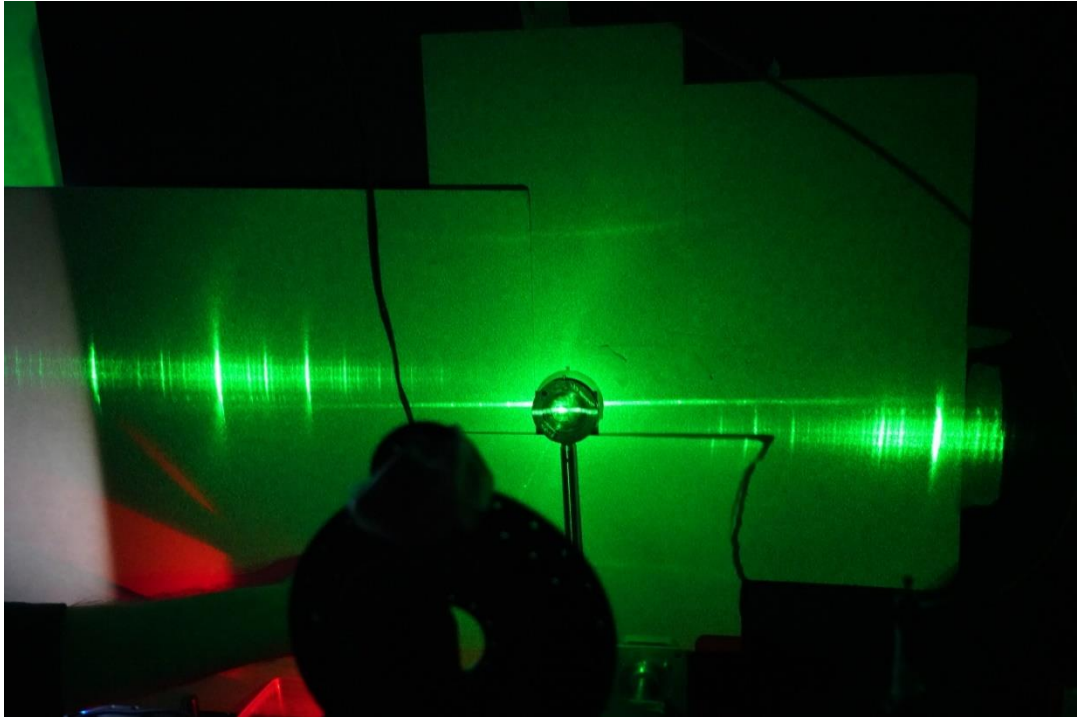


*Figure 4.2 Angle resolved scattering and the diffraction pattern of the grating processed by LIPSS on Ti surface.*

After SEM images are taken angle resolved scattering measurement is done. It gives the all tracks of laser induced the surface Figure 4.5. As it is seen in the Figure 4.5 surface morphology can be analyzed optically by the method. Laser light in p-polarization is sent to sample through the aperture. Firstly, middle scattered line refers to laser hatch lines which show up as intense dots in the red circles in the photograph. Their period is calculated about  $5 \mu\text{m}$  which matches with the laser hatching period that we attend during the experiment of LIPSS. There is an off axis between laser hatch line and grooves direction which agrees with the experiment. Also, the grooves are aligned perpendicular to the laser scanning direction. Also, overlapping period can be seen in the photograph which is shown via red arrows. And the intense fringes on the screen shown by the purple arrows correspond to grooves periods. Because of the grooves' periodic structure

laser light is resolved into angular modes and diffraction pattern of the grating is emerged related with the equation [49]

$$\Lambda \sin(\Theta_m) - \sin(\Theta_i) = m\lambda \quad (4.2)$$

Where  $\Lambda$  is the spacing between the grating grooves  $\Theta_m$  is the angle of the particular mode at which laser light is separated,  $\Theta_i$  is the incidence angle,  $m$  is the mode of scattering which is an integer number,  $\lambda$  is the wavelength of the laser used which is 532 nm.

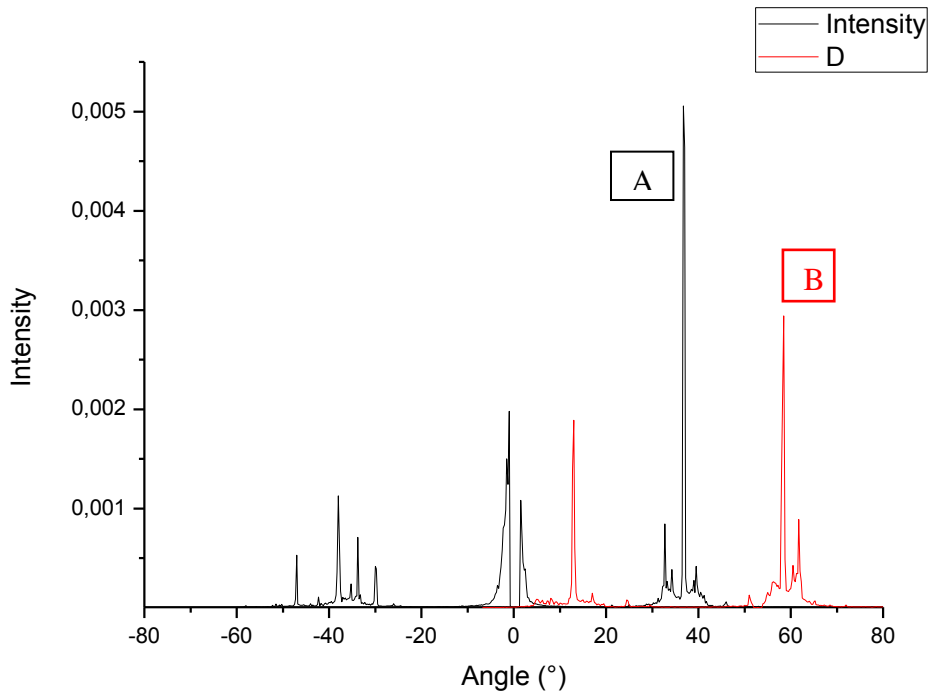


*Figure 4.3 Reflection of laser from the grating structured surface by LIPSS. Line A is normal incidence used for finding the period of the grating and Line B refers to reflection with 20° incidence angle.*

Also, period is calculated as 905 nm by substituting obtained results seen on the graph into the equation (4.2) which agrees with the SEM measurement which gave 909 nm as it is seen in the Figure 4.7.

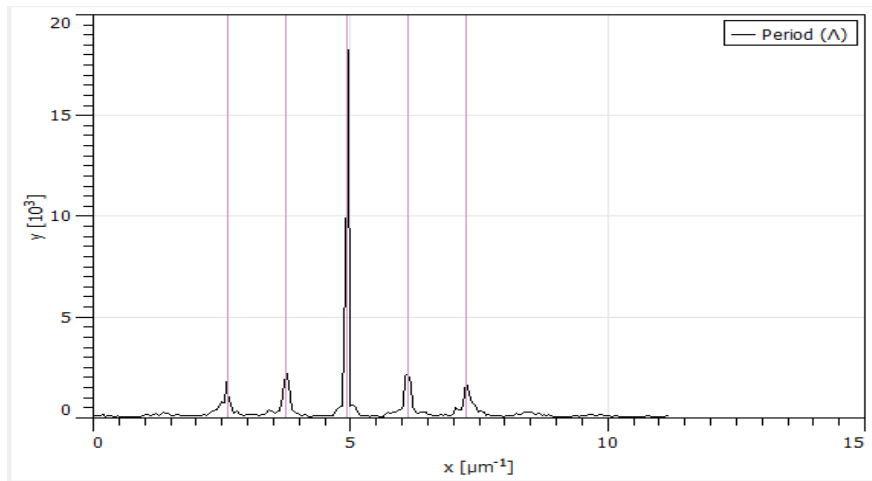
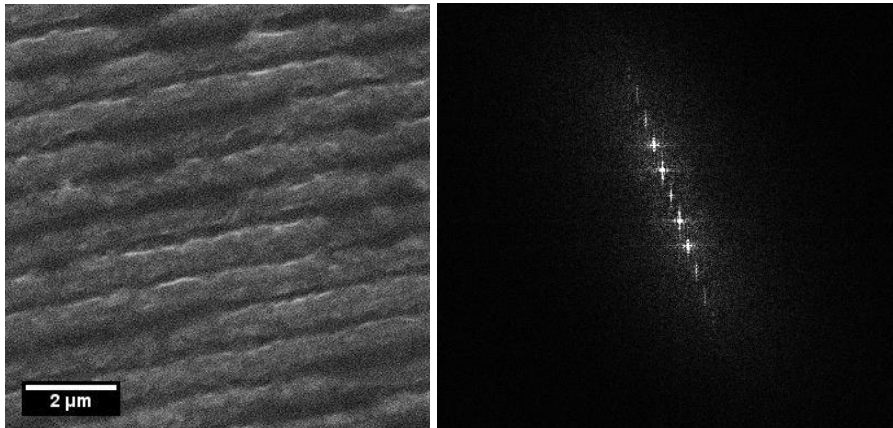


*Figure 4.4 The periods found via Gwyddion Software*

### 4.3 RAMAN

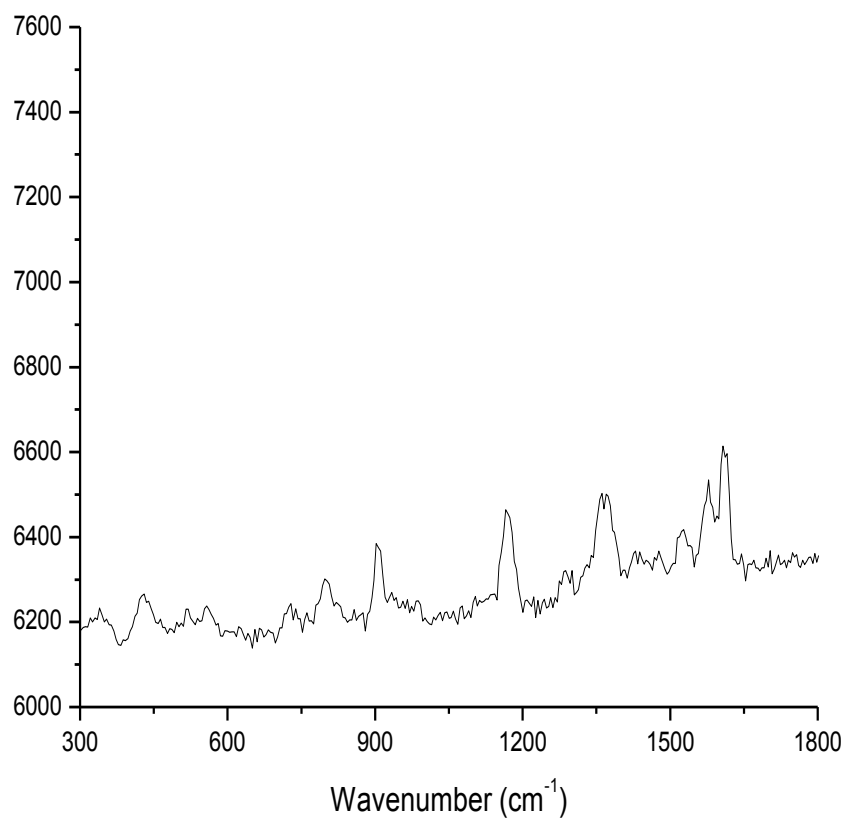


*Figure 4.5 Raman spectrum of  $10^{-4}$  M CV liquid droplet on Si wafer*

Whenever the laser wavelength is close to the absorption spectrum of the dye molecule, the enhancement is observed effectively. In the experiment CV molecule is a proper choice as it seen in the graph *Figure 4.5*

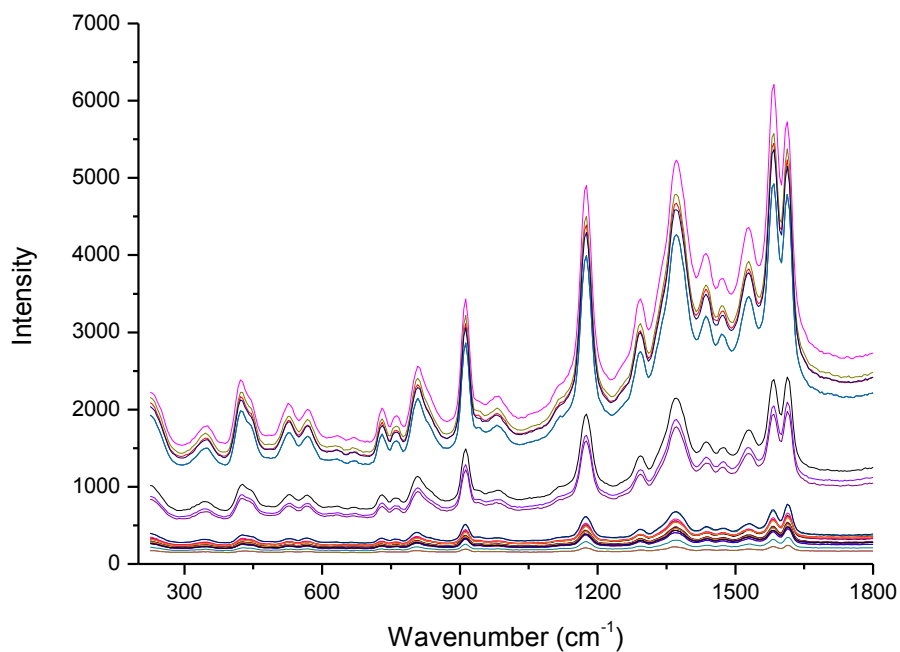


*Figure 4.6 Peak area around  $1350\text{ cm}^{-1}$  used for calculation of the CV dye molecule used SERS intensity spectra of Mo grating surfaces coated by Ag film. Exposure time 5 s and accumulation is 10.*

The surface enhanced Raman spectroscopy graph of 20 nm silver thin film coated over LIPSS applied 400 nm thick Mo samples is exhibited in *Figure 4.6*. Mo surfaces are processed under the power 350 mW and 700 mW. The scanning speed of laser is between 200 mm/s and 700 mm/s. Considering wavenumber of  $1350\text{ cm}^{-1}$  more intense Raman signal is obtained for 400 mW power and around 600 mm/s scanning speed.

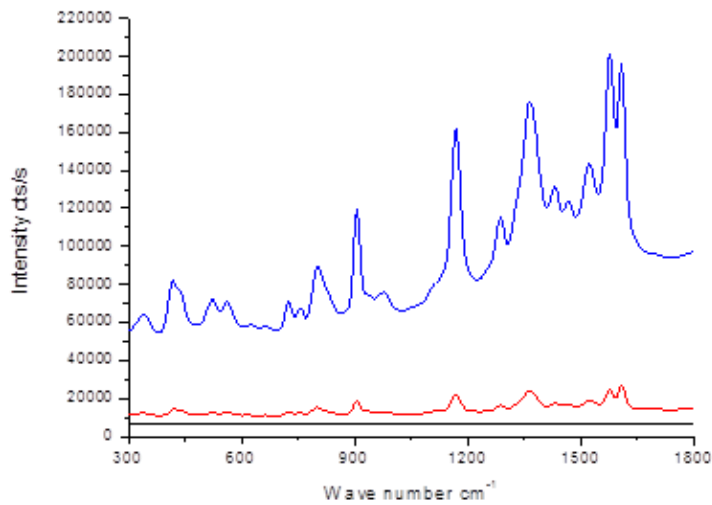


*Figure 4.7 Enhancement of 20 nm Ag thin films on LIPSS applied 400 nm thick Mo surface*

For a reference is needed to observe the relative enhancement, a substrate is prepared in the same condition with the ones used in the Raman measurement of the samples in Figure 4.6. But, the reference substrate is not coated by a silver layer and has not structured Mo layer. It is dyed by CV molecule solution which has the same molarity ( $10^{-4}$  M) and volume ( $20 \mu\text{L}$ ). It is understood from the Figure 4.7 that there is field enhancement. Therefore, according to enhancement factor equation (2.35), comparing the intensity, that is area under the peak of  $1359 \text{ cm}^{-1}$ , gives the relative intensity of Raman signal generated by the substrates with respect to the reference substrate.

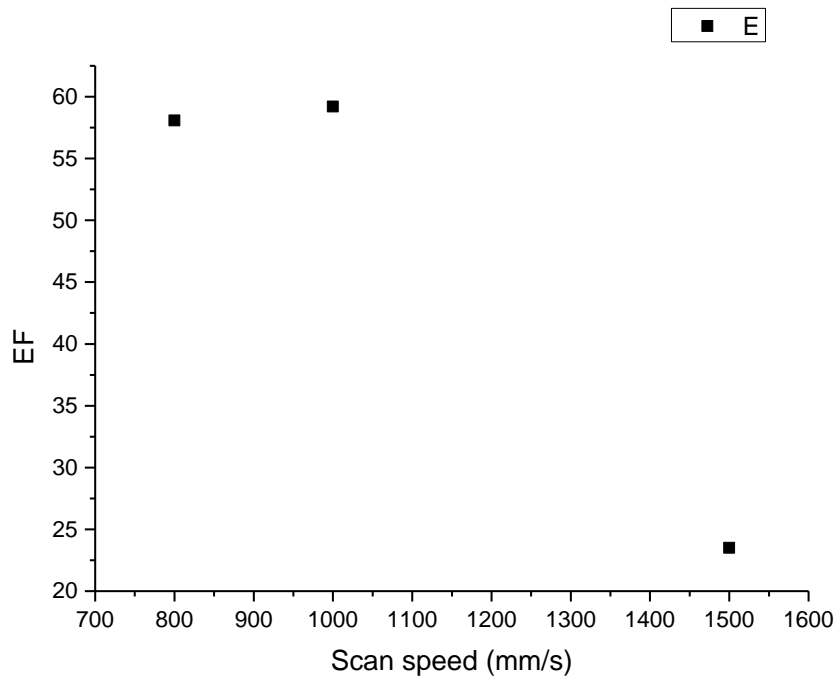


Figure 4.8 *Variously structured Mo surfaces, most powerful signal obtained in larger band correspond to more roughened surface considering the scanning speed.*

In the graph above relative enhancements of the samples are seen. The sample with lower power as 350 mW and lower scan speed as 100 mm/s shows powerful signal. As power increases to 600 mW 6 times greater scanning speed which is 600 mm/s gives the best result. But there is no straightforward relation increase power and speed to obtain optimized structure for the enhancement. When power increased to 400 mW from 300 mW no effective signal is observed in any scanning speed.



## CHAPTER 5

### CONCLUSION

400 nm thick Mo surfaces processed with LIPSS under central wavelength 1032 nm and a repetition rate of 1MHz of laser. Mo surface is found to have peirodicity of about 900 nm which is close to wavelentgh of laser. Thus, LSFL structures are obtained and SPP excitation mechanism is found to responsible mechanism of formation. The structures are analyzed optically with ARS as well as SEM. Structures are found in the same periodicty in both. Owing to ARS all tracks done by the laser can be screened. This method is found indispensable optical tool for the LIPSS especially reflective and tranmissive properties is concerned. To observe the another use of LIPSS which is generating effective SERS substrate, Raman spectroscopy of Mo is obtained. 20 nm thick silver coated Mo surfaces processed by LIPSS under the 350 mW power and spin coated of  $10^{-4}$  M solution of CV over the silver thin film.enhanced the Raman signal of 532 nm wavelentgh and 0.2 mW power laser.



## REFERENCES

- [1] H. Joerg, "Surfing the wave," *Nature*, vol. 461, no. October, pp. 720–722, 2009.
- [2] D. Pines, "Collective energy losses in Solids," *Rev. Mod. Phys.*, vol. 28, no. 3, pp. 184–199, 1956.
- [3] M. Fleischmann, P. J. Hendra, and A. J. McQuillan, "Raman spectra of pyridine adsorbed at a silver electrode," *Chem. Phys. Lett.*, vol. 26, no. 2, pp. 163–166, 1974.
- [4] R. H. Ritchie, "Plasma Losses by Fast Electrons in Thin Films," *Phys. Rev.*, vol. 106, no. 5, pp. 874–881, 1957.
- [5] D. L. Jeanmaire and R. P. VAN Duyne, "Surface Raman Spectroelectrochemistry Part1. Heterocyclic," *J. Electroanal. Chem.*, vol. 84, pp. 1–20, 1977.
- [6] S. Kawata, Y. Inouye, and P. Verma, "Plasmonics for near-field nano-imaging and superlensing," *Nat. Publ. Gr.*, vol. 3, no. 7, pp. 388–394, 2009.
- [7] H. F. Ghaemi and T. Thio, "Extraordinary optical transmission through sub-wavelength hole arrays," *Nature*, vol. 391, pp. 667–669, 1998.
- [8] W. L. Barnes, A. Dereux, and T. W. Ebbesen, "Surface plasmon subwavelength optics," *Nature*, vol. 424, pp. 824–830, 2003.
- [9] E. Verhagen, M. Spasenovic, A. Polman, and L. K. Kuipers, "Nanowire Plasmon Excitation by Adiabatic Mode Transformation," *Phys. Rev. Lett.*, vol. 102, no. 203904, pp. 1–4, 2009.
- [10] M. I. Stockman, L. N. Pandey, and T. F. George, "Inhomogeneous localization of polar eigenmodes in fractals," vol. 53, no. 5, pp. 2183–2186, 1996.
- [11] M. I. Stockman, "Nanoplasmonics: past, present, and glimpse into future," *Opt. Express*, vol. 19, no. 22, pp. 22029–22106, 2011.
- [12] A. Bek, R. Jansen, M. Ringler, S. Mayilo, T. A. Klar, and J. Feldmann, "Fluorescence enhancement in hot spots of AFM-designed gold nanoparticle sandwiches," *Nano Lett.*, vol. 8, no. 2, pp. 485–490, 2008.
- [13] B. Sharma, R. R. Frontiera, A. Henry, E. Ringe, and R. P. Van Duyne, "SERS : Materials , applications , and the future," *Mater. Today*, vol. 15, no. 1–2, pp. 16–25, 2012.
- [14] J. N. Anker, W. P. Hall, O. Lyandres, N. C. Shah, J. Zhao, and R. P. Van Duyne, "Biosensing with plasmonic nanosensors," vol. 7, no. June, pp. 8–10, 2008.
- [15] S. Greco, S. D. Zilio, A. Bek, M. Lazzarino, and D. Naumenko, "Frequency Modulated Raman Spectroscopy," 2018.
- [16] R. Buividas, P. R. Stoddart, and S. Juodkazis, "Laser fabricated ripple substrates for surface-enhanced Raman scattering," *Ann. Phys.*, vol. 524, no. 11, pp. 5–10, 2012.
- [17] M. Birnbaum, "Semiconductor Surface Damage Produced by Ruby Lasers,"

- J. Appl. Phys.*, vol. 36, no. 3688, pp. 1–3, 1965.
- [18] I. Pavlov, S. Ilday, H. Kalaycıog, A. Rybak, and S. Yavas, “Nonlinear laser lithography for indefinitely large- area nanostructuring with femtosecond pulses,” vol. 7, no. October, pp. 897–901, 2013.
- [19] J. Bonse, S. Hohm, S. V. Kirner, A. Rosenfeld, and J. Kruger, “Laser-Induced Periodic Surface Structures-A Scientific Evergreen,” *IEEE J. Sel. Top. Quantum Electron.*, vol. 23, no. 3, 2017.
- [20] A. Y. Vorobyev and C. Guo, “Femtosecond laser blackening of platinum Femtosecond laser blackening of platinum,” *J. Appl. Phys.*, vol. 104, no. 053516, pp. 1–4, 2008.
- [21] T. J.-Y. Derrien, J. Krüger, T. E. Itina, S. Höhm, A. Rosenfeld, and J. Bonse, “Rippled area formed by surface plasmon polaritons upon femtosecond laser double-pulse irradiation of silicon,” *Opt. Express*, vol. 21, no. 24, p. 29643, 2013.
- [22] Y. Fuentes-Edfuf, J. A. Sánchez-Gil, C. Florian, V. Giannini, J. Solis, and J. Siegel, “Surface Plasmon Polaritons on Rough Metal Surfaces: Role in the Formation of Laser-Induced Periodic Surface Structures,” *acs omega*, vol. 4, pp. 6939–6946, 2019.
- [23] S. Nie and S. R. Emory, “Probing Single Molecules and Single Nanoparticles by Surface-Enhanced Raman Scattering,” vol. 275, no. 5303, pp. 1102–1106, 1997.
- [24] D. J. Griffiths, *Introduction to Electrodynamics*, 3rd ed. New Jersey: Prentice Hall, 1999.
- [25] W. T. Silfvast, *Laser Fundamentals*, 2nd ed. Cambridge: Cambridge University Press, 2003.
- [26] E. Le Ru and P. Etchegoin, *Principles of Surface Enhanced Raman Spectroscopy*. Elsevier Ltd, 2009.
- [27] S. A. Maier, *Plasmonics: Fundamentals and Applications*. Springer, 2007.
- [28] M. Kauranen and A. V. Zayats, “Nonlinear plasmonics,” *Nat. Photonics*, vol. 6, no. 11, pp. 737–748, 2012.
- [29] D. Naumenko, V. Toffoli, S. Greco, S. Dal Zilio, A. Bek, and M. Lazzarino, “A micromechanical switchable hot spot for SERS applications,” *Appl. Phys. Lett.*, vol. 109, no. 13, 2016.
- [30] S. Postaci, B. C. Yildiz, A. Bek, and M. E. Tasgin, “Silent enhancement of SERS signal without increasing hot spot intensities,” *Nanophotonics*, vol. 7, no. 10, pp. 1687–1695, 2018.
- [31] L. G. Wang, S. Qamar, S. Y. Zhu, and M. S. Zubairy, “Manipulation of the Raman process via incoherent pump, tunable intensity, and phase control,” *Phys. Rev. A - At. Mol. Opt. Phys.*, vol. 77, no. 3, pp. 1–9, 2008.
- [32] X. Hua, D. V. Voronine, C. W. Ballmann, A. M. Sinyukov, A. V. Sokolov, and M. O. Scully, “Nature of surface-enhanced coherent Raman scattering,” *Phys. Rev. A - At. Mol. Opt. Phys.*, vol. 89, no. 4, pp. 1–7, 2014.
- [33] D. Dufft, A. Rosenfeld, S. K. Das, R. Grunwald, and J. Bonse, “Femtosecond laser-induced periodic surface structures revisited: A comparative study on ZnO,” *J. Appl. Phys.*, vol. 105, no. 3, pp. 1–37, 2009.

- [34] E. Rebollar, M. , Castillejo, and A. Ezquerro, Tiberio, “Laser induced periodic surface structures on polymer films: from fundamnetals to applications,” *Eur. Polym. J.*, vol. 73, pp. 162–174, 2015.
- [35] D. C. Emmony, R. P. Howson, and L. J. Willis, “Laser mirror damage in germanium at 10.6  $\mu\text{m}$ ,” *Appl. Phys. Lett.*, vol. 23, no. 11, pp. 598–600, 1973.
- [36] F. Keilmann and Y. H. Bai, “Periodic surface structures frozen into CO2 laser-melted quartz,” *Appl. Phys. A Solids Surfaces*, vol. 29, no. 1, pp. 9–18, 1982.
- [37] J. E. Sipe, J. F. Young, J. S. Preston, and H. M. van Driel, “Laser-induced periodic surface structure. I. Theory,” *J. Chem. Inf. Model.*, vol. 53, no. 9, pp. 1689–1699, 1983.
- [38] N. Wu *et al.*, “Nano-periodic structure formation on titanium thin film with a Femtosecond laser,” *J. Ceram. Soc. Japan*, vol. 119, no. 1395, pp. 898–901, 2011.
- [39] X. Sedao *et al.*, “Growth Twinning and Generation of High-Frequency Surface Nanostructures in Ultrafast Laser-Induced Transient Melting and Resolidification,” *ACS Nano*, vol. 10, no. 7, pp. 6995–7007, 2016.
- [40] S. Höhm, A. Rosenfeld, J. Krüger, and J. Bonse, “Laser-induced periodic surface structures on titanium upon single- and two-color femtosecond double-pulse irradiation,” vol. 23, no. 20, pp. 25959–25971, 2015.
- [41] F. Garrelie *et al.*, “Evidence of surface plasmon resonance in ultrafast laser-induced ripples,” vol. 19, no. 10, pp. 9035–9043, 2011.
- [42] A. Ancona *et al.*, “Femtosecond and picosecond laser drilling of metals at high repetition rates and average powers,” *Opt. Lett.*, vol. 34, no. 21, p. 3304, 2009.
- [43] M. Huang, F. Zhao, Y. Cheng, N. Xu, and Z. Xu, “Origin of laser-induced near-subwavelength ripples: Interference between surface plasmons and incident laser,” *ACS Nano*, vol. 3, no. 12, pp. 4062–4070, 2009.
- [44] I. Pavlov, O. Yavuz, G. Makey, O. Tokel, and O. Ilday, “Switching between normal and anomalous Laser Induced Periodic Surface Structures,” pp. 1–7.
- [45] G. D. Tsibidis *et al.*, “Modelling periodic structure formation on 100Cr6 steel after irradiation with femtosecond-pulsed laser beams,” *Appl. Phys. A Mater. Sci. Process.*, vol. 124, no. 1, p. 0, 2018.
- [46] H. Raether, *Surface Plasmons*. Springer-Verlag Berlin Heidelberg.
- [47] G. D. Tsibidis, M. Barberoglou, P. A. Loukakos, E. Stratakis, and C. Fotakis, “Dynamics of ripple formation on silicon surfaces by ultrashort laser pulses in subablation conditions,” *Phys. Rev. B - Condens. Matter Mater. Phys.*, vol. 86, no. 11, pp. 1–14, 2012.
- [48] M. Garcia-Lechuga, D. Puerto, Y. Fuentes-Edfuf, J. Solis, and J. Siegel, “Ultrafast Moving-Spot Microscopy: Birth and Growth of Laser-Induced Periodic Surface Structures,” *ACS Photonics*, vol. 3, no. 10, pp. 1961–1967, 2016.
- [49] “Hecht Eugene - Optics-Springer\_Verlag (2002).” .



